Chinese Journal of Chemical Engineering 23 (2015) 615–622

Contents lists available at ScienceDirect

Chinese Journal of Chemical Engineering

journal homepage: www.elsevier.com/locate/CJChE

Fluid Dynamics and Transport Phenomena

Influence of impeller diameter on local gas dispersion properties in a sparged multi-impeller stirred tank☆

Yuyun Bao, Jie Yang, Bingjie Wang, Zhengming Gao *

State Key Laboratory of Chemical Resource Engineering, School of Chemical Engineering, Beijing University of Chemical Technology, Beijing 100029, China

ARTICLE INFO

Available online 27 December 2014

Keywords:
Impeller diameter
Local void fraction
Bubble size
CFD-PBM
Mixing

ABSTRACT

Vertical distributions of local void fraction and bubble size in air–water dispersion system were measured with a dual conductivity probe in a fully baffled dished base stirred vessel with the diameter T of 0.48 m, holding 0.134 m^3 liquid. The impeller combination with a six parabolic blade disk turbine below two down-pumping hydrofoil propellers, identified as PDT + 2CBY, was used in this study. The effects of the impeller diameter D, ranging from 0.30T to 0.40T (corresponding to D/T from 0.30 to 0.40), on the local void fraction and bubble size were investigated by both experimental and CFD simulation methods. At low superficial gas velocity V_S of 0.0077 $m \cdot s^{-1}$, there is no obvious difference in the local void fraction distribution for all systems with different D/T. However, at high superficial gas velocity, the system with a D/T of 0.30 leads to higher local void fraction than systems with other D/T. There is no significant variation in the axial distribution of the Sauter mean bubble size for all the systems with different D/T at the same gas superficial velocity. CFD simulation based on the two-fluid model along with the population balance model (PBM) was used to investigate the effect of the impeller diameter on the gas–liquid flows. The local void fraction predicted by the numerical simulation approach was in reasonable agreement with the experimental data.

1. Introduction

Gas–liquid stirred reactors offer unmatched flexibility and control to tailor the fluid dynamics, which is the reason why they are widely used in the chemical, mineral, and biochemical industries, wastewater treatment, *etc.* With the increasing industrial scope, large gas–liquid reactors are widely used, so that it becomes more important to optimize the mixing reactors design. For example, the size of reactors like fermentors can be as large as 800 m^3, leading to the aspect ratio of vessels significantly greater than one, and therefore the requirement of multiple impeller agitators for mixing and dispersion in such vessels [1–4]. During the last two decades, more and more studies were carried out in systems with multiple impellers [5–11]. The study of stirred tanks with single or double impellers has been unable to meet the needs of the industrial design. In a stirred tank agitated by multiple impellers, the flow pattern can be significantly changed for the flow interactions between the impellers, heavily dependent upon the configurational parameters such as impeller spacing and impeller sizing [12]. However, in stirred tanks with multiple-impeller, the study of the impeller diameter optimization is rarely reported.

In large scale industrial gas–liquid reactors, the manufacturing and operational costs are closely related to the optimal design parameters of the impeller, especially the diameter of impellers. Given the same power input of the reactors, the impellers with smaller diameter have higher rotational speed and less torque compared with the larger diameter impellers. As a result, the size of the gearing box, mechanical seals, and impeller shaft are determined by the choice of the impeller diameter, which becomes very important in large scale reactors with a volume up to 800 m^3. In recent years, there are some studies only focusing on the macroscopic gas–liquid dispersion [13,14]. Therefore, further research is needed to investigate the relationship between the local gas dispersion properties and the agitator geometrical parameters, to provide the data for optimizing the design of agitators.

The limitations in measurement techniques lead to the lack of local information in multi-impeller gas–liquid stirred tanks. In recent decades, more and more measurement techniques were used such as capillary probes, conical hot-film probes and conductivity probes. Among those measurement techniques, the conductivity probe is a method suitable for both opaque and dense dispersions. The limitation is that the size of the probe tip determines the minimum bubble size which can be detected.

During the last two decades, computational fluid dynamics (CFD) techniques have been used to calculate hydrodynamics in stirred tanks [11,15–20]. Compared with the experimental measurements, CFD technique is more efficient and convenient to study the effect of impeller parameters on the gas–liquid flow. Moreover, CFD technique can

☆ Supported by the National Natural Science Foundation of China (21121064, 21206002, 21376016).
* Corresponding author.
E-mail address: gaozm@mail.buct.edu.cn (Z. Gao).

http://dx.doi.org/10.1016/j.cjche.2014.12.006
1004-9541/

also reveal the details that cannot be easily measured in experiments, such as the distribution of the local void fraction in the impeller discharging region. Thus, the application of CFD simulation has important significance in the investigation of gas–liquid flow in multi-phase stirred tanks.

In the present study, a turbine-propeller combination consisted of a parabolic blade disk turbine below two down-pumping hydrofoil propellers, identified as PDT + 2CBY, was used. The macroscopic gas–liquid dispersion properties are not sufficient to optimize the industrially important aerated vessels with multiple impeller agitators, so this study is focused on the local gas dispersion properties. Our objective is to obtain the vertical profiles of local void fraction and bubble size distributions in an aerated vessel with multiple impeller agitators. The CFD simulation was also used to predict the local gas dispersion properties in the multi-impeller stirred tank.

2. Experimental Setup

All the experiments were carried out in a dished-bottom cylindrical tank with an internal diameter T of 0.48 m and a liquid-filling aspect ratio H/T of 1.66, as sketched in Fig. 1. The geometry of the tank was exactly the same as that used in our previous studies [5,8–10]. The bottom impeller is a disk turbine with six parabolic blades, the middle and upper impellers are down-pumping hydrofoil propellers, and the configuration is identified as PDT + 2CBY [Fig. 2]. The impeller diameter D of the combinations was 0.30T, 0.33T, 0.37T, and 0.40T. For each impeller combination, PDT and two CBYs had the same impeller diameter. The distance between neighbor impellers was 0.48T. The clearance between the lowest impeller and the base of the tank was 0.33 T. A ring sparger of 0.8D was located 0.25T above the tank bottom and with 27 holes whose diameter was 2 mm. Four baffles each 0.045 m wide were mounted 0.005 m away from the wall.

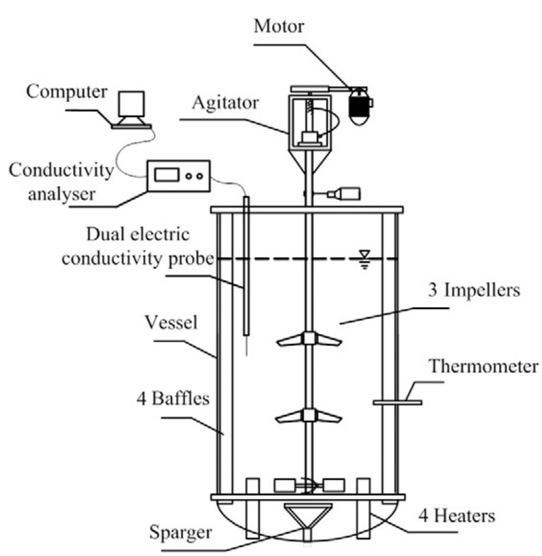

Fig. 1. Schematic of the experimental setup.

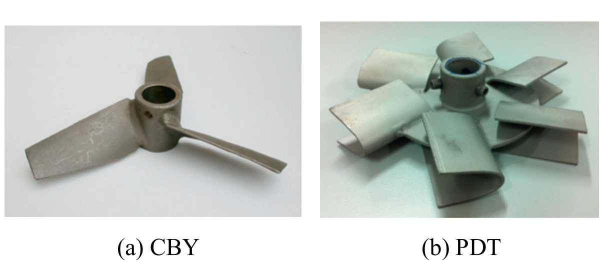

Fig. 2. Impellers.

Air and deionized water were used as the gas and liquid phases in all experiments. In order to enlarge the conductivity difference between deionized water and air, 3 ml phosphoric acid was added in the deionized water. We measured the interfacial tension of the water before and after the phosphoric acid was added, and they were 0.07408 and 0.07355 $N\cdot m^{-1}$, respectively, with the relative error of 0.7%. And the total gas holdups measured before and after the phosphoric added were the same, so it is believed that the impact of phosphoric acid on the coalescence property of water can be neglected. Air passed through three-stage filters before being sparged into the tank in order to get rid of the impurities in gas. The total gas rates ranged from 5 to 25 $m^3\cdot h^{-1}$, and the corresponding superficial velocities were from 0.0077 to 0.0385 $m\cdot s^{-1}$, respectively. The liquid bulk temperature was kept constantly at 25 °C.

The distributions of the local void fraction and the bubble size were measured by using a dual electric conductivity probe which was co-developed with the Institute of Process Engineering of the Chinese Academy of Sciences, as shown in Fig. 3.

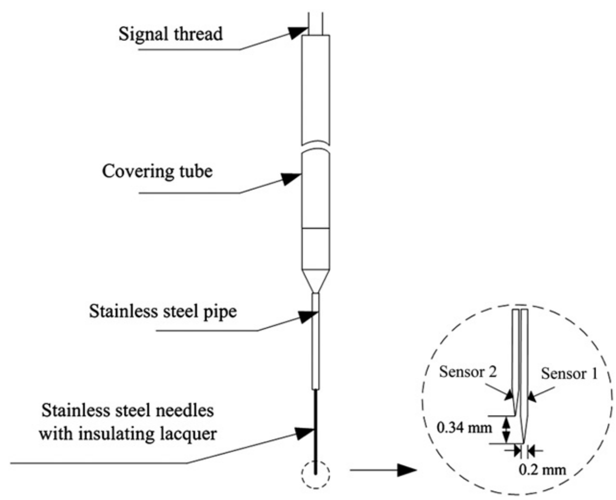

Fig. 3. Construction of dual electric conductivity probe.

When the probe was in the gas phase, the measurement circuit was open, and a high-voltage signal was the output. While the probe was in the liquid phase, the circuit was close, and resulted in a low-voltage output. After the signals passed through amplifier, rectifier, and smoothing circuits, square-wave signals were generated, as shown in Fig. 4.

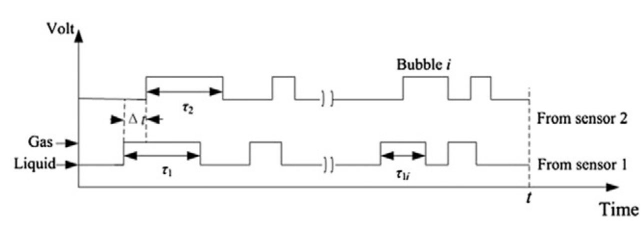

Fig. 4. Processed output signals from dual electric conductivity probe.

The gas-to-liquid ratio in a heterogeneous mixture passing through a specific point in a reactor was proportional to the ratio between the passage time of all the bubbles and the total sampling time. The time-averaged quantity of the local void fraction, ε, was given by

$$\varepsilon = \frac{\sum_{i=1}^{i=n_b} t_{gi}}{t} \tag{1}$$

where t_{gi} is the passage time of the ith bubble; n_b is the number of bubbles in the sample; and t is the total sampling time. A sampling rate of